ISSN Print: 2664-6536
ISSN Online: 2664-6544
Impact Factor: RJIF **5.4**
IJBB 2024; 6(1): 89-101
www.biosciencejournal.net
Received: 05-02-2024
Accepted: 10-03-2024

Mohammed Aqeel Abdulrazzaq
Department of Biology, College of Education, Qurnah University of Basrah, Basrah, Iraq

Ismaal Jmia Abas
Department of Biology, College of Education, Qurnah University of Basrah, Basrah, Iraq

Corresponding Author:
Ismaal Jmia Abas
Department of Biology, College of Education, Qurnah University of Basrah, Basrah, Iraq

Anti-biofilm and antibacterial activities of silver nanoparticles synthesized by using *Pseudomonas aeruginosa*

Mohammed Aqeel Abdulrazzaq and Ismaal Jmia Abas

DOI: https://dx.doi.org/10.33545/26646536.2024.v6.i1b.68

Abstract
A number of soil samples were collected from the escarpment of the Euphrates River, north of the city of Basra, by digging the soil by 5 cm, taking a portion of the soil, storing it in a sterile plastic cup, and transporting it to the laboratory. The samples were diluted with distilled water and grown on nutrient agar medium. They were purified. Bacterial isolates were obtained by taking single isolates and cultivating them on the nutrient medium using a planning method. The process was repeated until single colonies were obtained. The bacterial isolate was identified as *Bacillus subtilis* by diagnosing it phenotypically, examining it under a microscope, and performing biochemical tests, in addition to using a technique. PCR using the 16SrRNA gene. The supernatant solution was treated with *B. subtilis* bacteria with a solution of silver nitrate at a concentration of 1 mM, the color variation of the reaction mixture occurred, which was considered preliminary evidence of the formation of silver nanoparticles. The AgNPs were characterized by examination with a UV-visible spectroscopy device, and an FTIR device was used to detect the presence of active groups that contributed to the stability of the AgNPs. An SEM and TEM device were used, and the examination results showed the surface nature and the dominant spherical shape, in addition to the size, at a rate of 25 nm. An XRD device was used, and the test results showed that the AgNPs had a crystalline form. An EDX device was used, and the results revealed the presence of peaks indicating silver. The ability of AgNPs to inhibit the growth of pathogenic bacteria represented by *Pseudomonas aeruginosa*, *E. coli*, and *Klebsiella. Pneumonia* and *Staphylococcus aureus* Using the etch diffusion method, the results showed that the AgNPs had a high ability to inhibit bacterial growth. A test was conducted to detect some virulence factors, such as catalase, and the effectiveness of silver nanoparticles in inhibiting them. The biofilm was detected by a microtiter plate, and the results showed the ability of the AgNPs to inhibit biofilm effectively.

Keywords: AgNPs, SEM, TEM, biofilm, microtiter plate, XRD, EDX, *Bacillus subtilis*

Introduction
Many pathogenic bacteria have become a major cause of many dangerous diseases, and with bacteria possessing many drug resistance mechanisms, the problem of multidrug resistance has been exacerbated by many negative and positive bacteria, due to the excessive and unregulated use of antibiotics in treating bacterial infections, which increased the spread of many bacterial strains with multiple resistance and the length of the treatment period, thus increasing the death rate [1]. Many studies have shown that medical and industrial materials that contain silver have an inhibitory effect against many bacterial strains and against many fungi and viruses Many studies have shown that silver nanoparticles eliminate bacteria at low concentrations without causing toxic effects on human cells [2]. This is what prompted researchers and scientists to take the path of biosynthesis of metals and minerals as alternatives to antibiotics for the purpose of reducing the risk of multiple bacterial resistance or as anti-virulence agents. Nanotechnology aims to manufacture and apply nano-sized materials (1-100 nm), as it has these nanoparticles have many unique chemical, physical, and biological properties. Many studies have proven that AgNPs kill bacteria without any toxic effects on human cells, in addition to the fact that silver nanoparticles have the characteristic of a large surface area compared to their size, which facilitates their attachment to functional aggregates, and their small size has enabled them to be used in many fields as anti-cancers and anti-bacterial infections [3, 4].

Many studies and research have demonstrated that AgNPs have the ability to inhibit many virulence factors, such as biofilm, and many enzymes produced by bacteria, such as catalase, hemolysin, and proteases [5, 6]. Many methods have been used to manufacture silver nanoparticles, including biological methods such as the use of plant extracts [7]. And fungi and many bacterial species synthesize nanoparticles from many metals, such as silver and gold [8, 9]. The use of chemical and physical methods to manufacture nanoparticles has been dispensed with because they are toxic to the environment and to humans and are economically expensive. On the contrary, biological methods have been distinguished in that they are highly productive, environmentally friendly, and non-toxic, in addition to being economically inexpensive [10]. Components of the cell wall, proteins, and enzymes secreted in the supernatant solution of bacteria were used in the biosynthesis process [11]. Many studies have proven the ability of *Bacillus subtilis* to carry out extracellular biosynthesis in its bacterial culture supernatant solution [12].

Materials and methods

Collecting and culturing samples

Soil samples were collected from the edge of the Euphrates River in northern Basra by taking a portion of the soil 5 cmdeep, storing it in a sterile plastic cube, and transporting it to the laboratory. The soil samples were diluted with distilled water by taking 1 g of soil and dissolving it in a test tube containing 5 ml. From sterile distilled water, the samples were grown on the nutrient medium using a cotton swab and incubated at a temperature of 37 °C [13].

Diagnosis of bacterial isolates

Bacterial isolates were diagnosed based on phenotypic characteristics by observing the shape of the colonies growing on the nutrient agar plate, in addition to staining them with Gram stain and examining them under the microscope to reveal their shape and cell arrangement, and biochemical tests were performed [14]. The bacterial isolate was diagnosed using PCR technology based on the 16S rRNA gene and detecting the size of the bands formed when the gene was amplified using electrophoresis of the resulting DNA [15].

Synthesis of silver nanoparticles using *B. subtilis*

The method of extracellular synthesis of silver nanoparticles was used. The bacterial suspension of *B. subtilis* bacteria was prepared and inoculated into 250 ml conical flasks containing 100 ml of sterile Nutrient Broth Medium. The flasks were incubated in a shaking incubator at a rotation speed of 150 rpm. At a temperature of 37 °C and for 48 hours, after the end of the incubation period, the bacterial cultures were centrifuged at a speed of 8000 rpm for 20 minutes, and the supernatant liquid of the bacteria was collected in sterile beakers. A silver nitrate solution was prepared by dissolving 0.169 grams of AgNO3. In 1 liter of distilled water to obtain a concentration of 1 mM then, 90 ml of silver nitrate solution was mixed with 10 ml of the supernatant solution of the bacterial culture in a 250 ml conical flask. The flasks were covered with an opaque material to prevent oxidation due to light, and the reaction mixture was incubated in the shaking incubator at a rotation speed of 150 rpm. At a temperature of 37 °C for 48 hours, the supernatant solution of *B. subtilis* bacteria was incubated without adding silver nitrate solution to it as a negative control agent After the end of the incubation period, the color changes of the reaction mixture were observed, which is preliminary evidence of the reduction of silver nitrate to silver nanoparticles, which indicates the presence of reducing agents in the supernatant solution of bacteria $Ag^{+} \rightarrow Ag^{0}$ [16].

Characterization of silver nanoparticles

Change in the color

After the end of the incubation period, the color variation of the reaction mixture was observed, which is considered a preliminary indication of the formation of silver nanoparticles as the color changes from pale yellow to brown or reddish brown [17].

UV-visible spectroscopy

The wavelength of the silver nanoparticles was measured by withdrawing 5 ml of the reaction mixture after the color change occurred, then it was exposed to an ultrasound device for 15 minutes, then it was measured with a UV-visible spectroscopy device, and the supernatant solution of bacteria was used to zero the device, and the measurement was made at a wavelength of 200. (1000 nm) [18].

Fourier transform infrared (FTIR) spectroscopy

This test was performed using an FTIR instrument, which helps to identify the active functional groups in the supernatant solution of the bacterial cultures that reduces the Ag ions to Ag NPs. This was done by preparing a mixture of nanomaterial with potassium bromide tablets, then preparing pellets with the mixture and entering the device and measuring the in within a range. (400-4000cm) [19].

Scanning electron microscope (SEM)

SEM analysis of the formed particles was conducted to show the surface of the sample by employing a scanning electron microscope wherein a precisely focused beam of electrons was used to scan the surface of the sample in order to obtain a microscopic picture of the silver nanoparticles besides verifying the homogeneity of the examined material [20].

Transmission electron microscope (TEM)

This device was utilized to decide the shape, size, and crystalline phase of the synthesized silver nanoparticles prepared at a voltage of 100 KV [21].

X-ray diffraction (XRD)

It was employed to ascertain structural characteristics of the prepared particles, as well as to get information about the crystal structure and surface morphology of the prepared particles using Shimadzu 600 type device with using monochromatic copper beam of 0. In its operation, it was 15406 nm (4 kV) with a working current of 30 amps, scanning speed of 0. 02 degrees within an angular range of 2 Ɵ, and an entry hole for rays with a diameter of 0. 3 mm. The material being examined was in form of powder which was spread on a tape having a silicon base [22].

Energy diffraction X-ray (EDX)

Measurements this test was conducted using EDX by using an EOL JSM 7600 F to detect silver nanoparticles [23].

The effect of silver nanoparticles on the growth of pathogenic bacteria

Several concentrations of silver nanoparticles were prepared by dissolving (0.001 g) of AgNPs, which were diluted to obtain the concentrations (25 µg\ml-50 µg\ml-75 µg\ml-100 µg\ml) according to [24]. Four pathogenic bacterial species isolated from pathological cases were used to conduct testing on them: *P. aeruginosa*, *E. coli*, *K. pneumonia*, and *S. aureus*. They were grown on Muller-Hinton agar medium, and holes with a diameter of 6 mm were made. The concentrations were added to the holes (0.2 ml) and incubated in the incubator at a temperature of 37 °C for 24 hours. After the end of the incubation period, the diameters of inhibition were measured using a numbered ruler [25].

Prepare the minimum inhibitory concentration (MIC)

A set of sterile test tubes was prepared containing 1.8 ml of nutrient broth medium, and 0.1 ml of bacterial suspension was added to it. The concentrations (25 µg \ ml, 50 µg \ ml, 75 µg \ ml, and 100 µg \ ml) were added in an amount of 0.1 ml to The tubes were left with four tubes containing the culture medium and the bacterial suspension alone, without adding a solution of silver nanoparticles. They were considered negative control agents and were incubated in the incubator for 24 hours at a temperature of 37 °C. After the end of the incubation period, the minimum inhibitory concentration was determined by comparing its turbidity. Negative control test tubes with test tubes containing bacterial cultures and the concentration of silver nanoparticles, where the MIC was determined, which is considered the lowest concentration of silver nanoparticles that prevented the appearance of growth in the test tubes [26].

Effect of silver nanoparticles on catalase enzyme

This test was performed by culturing the pathogenic bacterial species *P. aeruginosa*, *E. coli*, *K. pneumonia*, and *S. aureus* in test tubes containing 1.8 ml of nutrient agar broth medium, and 0.1 ml of the minimum inhibitory concentration was added to four test tubes. Four test tubes containing the culture medium and the bacterial suspension were left as a negative control agent. The tubes were incubated in the incubator at a temperature of 37 °C for 24 hours. After the end of the incubation period, a few drops were taken from the treated and untreated bacterial cultures and placed on a glass slide. Sterilized, and a few drops of hydrogen peroxide solution (3%) were added to it, and it was observed whether bubbles appeared or not [27].

Effect of AgNPs on Biofilm Formation

Bacterial suspension was prepared for the four bacterial species that form the biofilm: *P. aeruginosa*, *E. coli*, *K. pneumonia*, and *S. aureus*, and they were transferred to test tubes containing nutrient broth containing glucose at a concentration of 2%. 0.08 ml of bacterial cultures were transferred. To drill a microtiter plate, a group of holes containing only the culture medium without the bacterial suspension and without a solution of silver nanoparticles were left as negative control factors. To compare the holes containing the culture medium and the bacterial suspension to measure the intensity of the biofilm, a group of silver nanoparticle concentrations was added. (25 µg\ml - 50 µg\ml - 75 µg\ml - 100 µg\ml) For the remaining holes, the plate was incubated in the incubator at a temperature of 37 °C for 24 hours. After the end of the incubation period, the microtiter plate was emptied of the bacterial cultures and washed with phosphate buffered saline (PBS) and left to dry at room temperature for 15 minutes. The holes were dyed with crystal violet dye and left for 15 minutes. After that, the contents of the holes were emptied and washed with a saline-phosphate buffer solution. Glacial acetic acid was added at a concentration of 33% and was measured with the ELISA device. The intensity of biofilm formation was measured by comparing the results of the negative control pits containing the culture medium only with the positive control pits containing the culture medium with the bacterial suspension of the bacterial samples, where AC symbolizes the negative control pits and A Positive control pits are represented by Table 1. The effect of silver nanoparticles on biofilm formation was calculated by applying the inhibition calculation equation, where the pits of the plate forming the biofilm were considered a negative control factor and the control pits containing silver nanoparticle concentrations were considered positive control factors [28].

Table 1: Shows the intensity of biofilm formation.

A ≤ AC	Non-biofilm forming
AC ≤ A ≤ 2 * AC	Medium biofilms
2 * AC ≤ A	Strong biofilms

$$\text{Inhibition of biofilm} = \frac{\text{Negative control wavelength} - \text{positive control Wavelength}}{\text{Negative control wavelength}} \times 100$$

Biofilm inhibition equation

Results and discussion

Collecting samples

Soil samples were collected from areas north of the city of Basra, on the edge of the Euphrates River. The samples were preserved in a plastic cube and transported to the laboratory. They were diluted with distilled water by weighing 1 gram and dissolving them in 5 ml of sterile distilled water. They were grown on nutrient agar medium, where *Bacillus subtilis* bacteria were isolated and purified by repeated cultivation until pure colonies were obtained.

Appearance characteristics of the colonies

Bacterial colonies appeared on the nutrient agar medium in a relatively large, circular shape with a smooth, rounded edge that turned into a lobed edge over time. The diameter of the colony ranged from 1.5 to 3.5 mm and was characterized by its white to brown color, as in The results Figure (1) were consistent with [29].

Fig 1: Showing the growth of *Bacillus subtilis* bacteria on nutrient agar medium

Microscopic diagnosis

The results of staining the bacterial colonies with Gram stain and examining them under the microscope showed that the bacterial cells had a rod-like shape of medium length and were positive for Gram stain. The results were consistent with [30].

Biochemical tests

Biochemical tests were performed on *Bacillus subtilis* bacteria, as shown in Table 2, and the results were consistent with [31, 32].

Table 2: Results of biochemical tests for *Bacillus subtilis*

Isolate	Indole	MRD	Catalase	Oxidase	Citrate	Urease
Bacillus	-	-	+	+	+	+

Molecular diagnosis: The molecular diagnosis of *Bacillus subtilis* bacteria was carried out using *16SrRNA.* The extraction results showed the appearance of DNA bands on the agarose gel. The results of DNA amplification through the PCR polymerase chain reaction showed that the size of the base pairs was (1500 bp) Figure (2) and (3) when using primers. Genes (F 27) and (R 1492), when comparing the size of the package with the DNA ladder as shown in Image (3), The Sanker technique was used to analyze the amplification product of the *16SrRNA* diagnostic gene for the bacterial isolate studied, and after conducting a BLAST search on the National Center for Biotechnology Information website, it appeared. The study isolate was 96% identical to the species It is available in GenBank, and the sequences of the particular bacterial isolate studied were recorded under the number PP273436. Table (3) [33, 35].

Table 3: Accession NO and the ancestry and matching percentage of the study sample

Closed blast match	Strain	Accession NO.	E-Value	Identity
Bacillus subtilis	M1Q1 16S ribosomal RNA	PP273436	0.0	96.40%

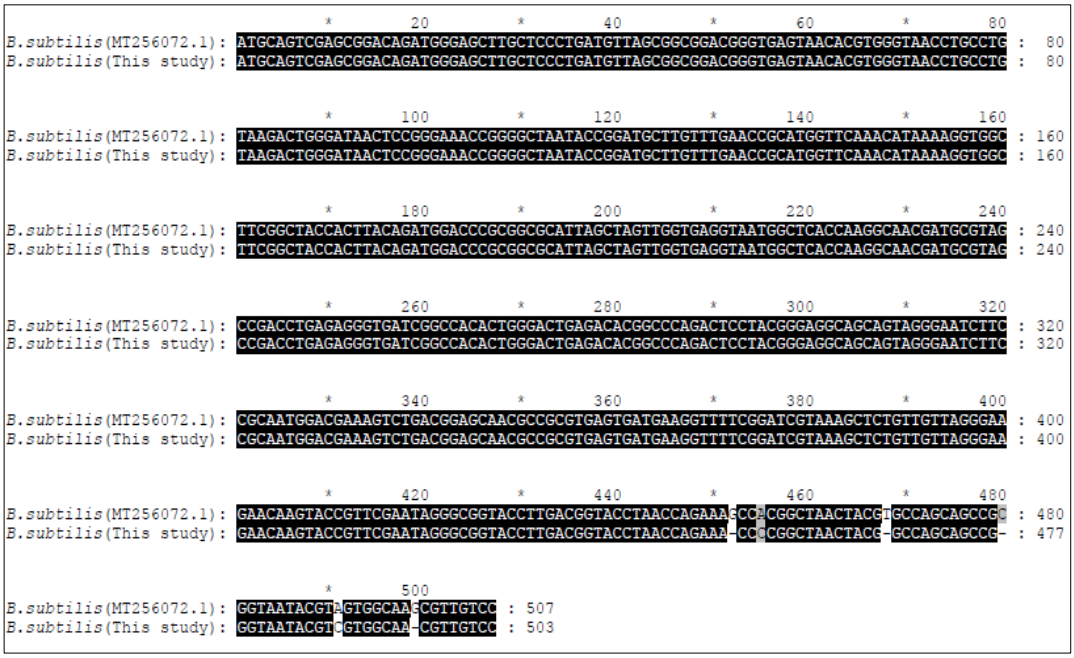

Fig 2: Accession NO and the ancestry and matching percentage of the study sample

Fig 3: DNA amplification of the current study sample

Characterization of AgNPs

Changing the color

After the end of the incubation period, the color variation of the reaction mixture consisting of 10 ml of *B. subtilis* bacterial suspension and 90 ml of $AgNO_3$ solution was observed.

When the color of the reaction mixture was compared with the color of the negative control flask that contained only the supernatant solution of the bacteria, as shown in Figure (4) It was observed that the color changed from yellow to brown, and this is a preliminary indication of the formation of silver nanoparticles, as stated in [35]. The appearance of the color of the reaction mixture in a color other than the bright silver color is due to surface plasmon resonance, which occurs due to the diameters of the particles reaching nano-sized diameters [36].

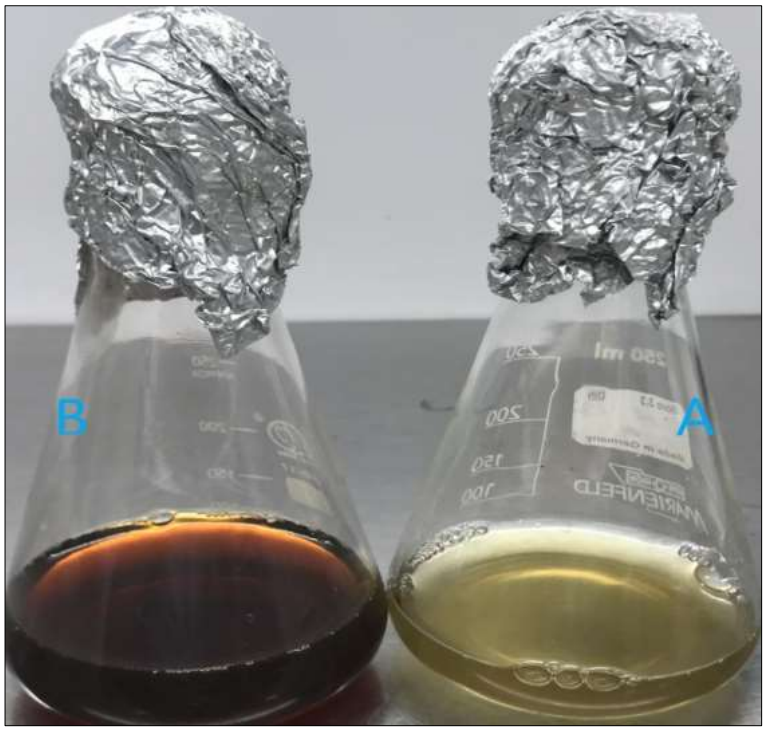

Fig 4: The bacterial supernatant was incubated with 10% of the supernatant and 1 mM of $AgNO_3$ before and after incubation for 48 h. The biosynthesis was confirmed by changing the color of the reaction as a visual indicator

Characterization of AgNPs UV-Vis spectrophotometer analysis

The results of the UV-Vis spectrophotometer analysis showed the appearance of an absorption peak at the wavelength (456 nm), as shown in Figures 1 and. Figure (5)

The image and figure showed the amount of absorbency of the silver nanoparticles, as the enzymes present in the supernatant solution of the bacteria played an important role in reducing silver ions and converting them into silver nanoparticles [37].

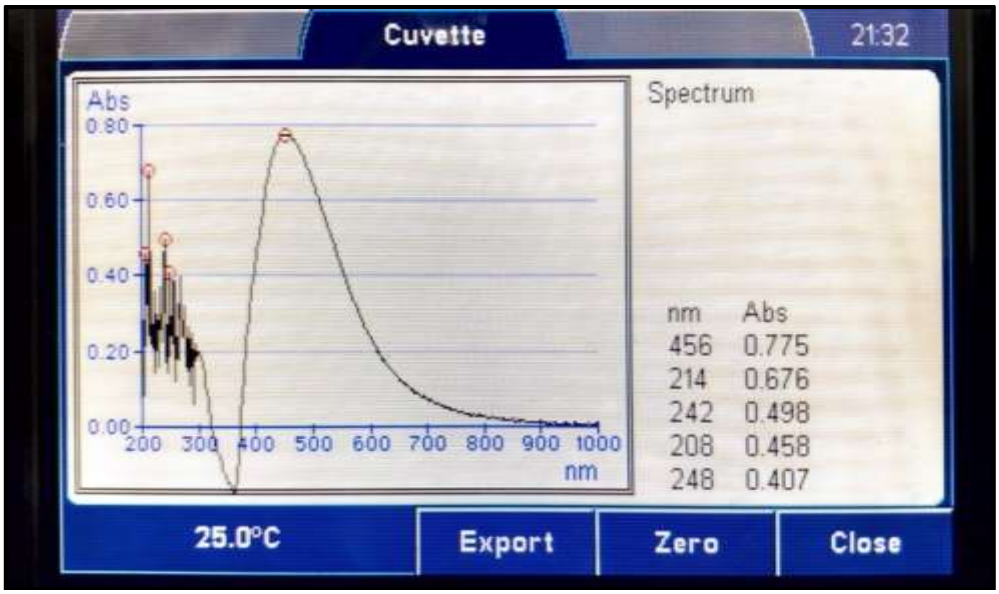

Fig 5: Is an absorption spectrum of silver nanoparticles in a device. UV-Vis spectrophotometer

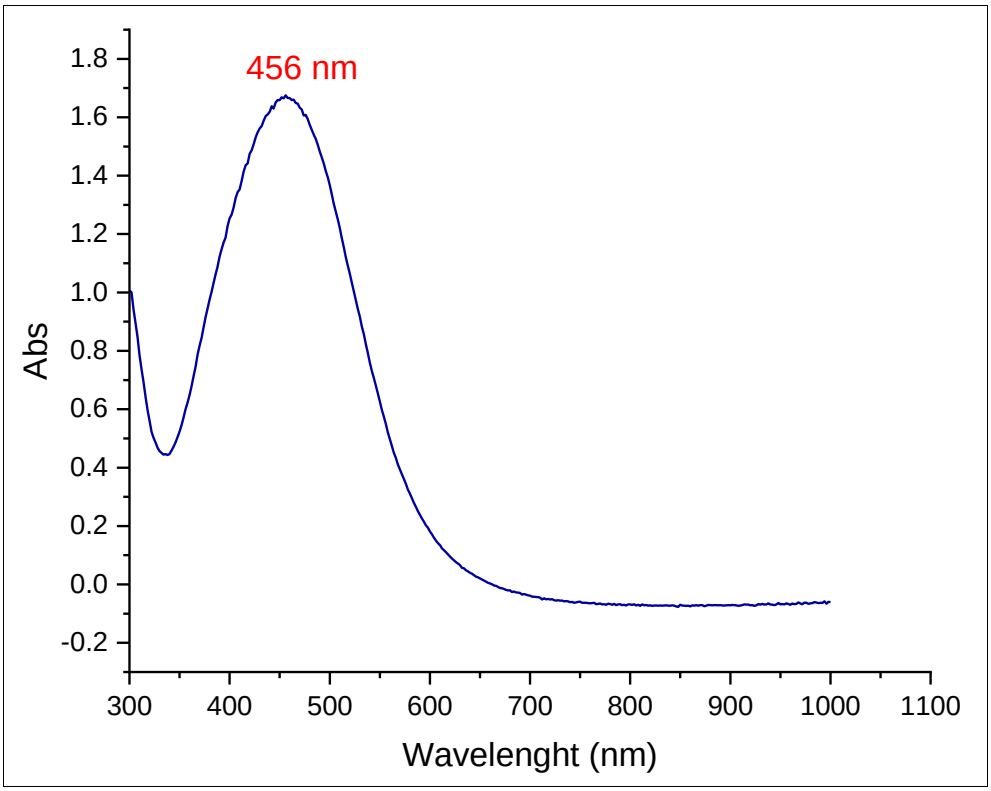

Fig 6: UV-vis absorbance curve of the reaction mixture after incubation. The maximum absorbance peak of surface plasmon of AgNPs present at 456 nm

Fourier transform-infrared (FT-IR) spectroscopy

The active groups contained in the supernatant solution of bacteria, which are responsible for reducing silver nitrate salts to silver nanoparticles, were detected. The results showed the appearance of an absorption peak at a wavelength of 2923.56 cm^{-1}, which indicates the presence of a C-H carboxyl bond in the alkane groups and a peak. Another peak at the wavelength of 1542.77 cm^{-1} indicates the presence of the N-O bond found in nitro compounds, in addition to another peak at the wavelength of 1396.21 cm^{-1}, which indicates the presence of the O-H hydroxyl bond found in carboxylic acids, and a peak at 1056.21 cm^{-1} indicates the C-O bond of carbon monoxide. Figure (7) shows the absorbance peaks in FT-IR. These results indicate the role played by the extracellular active groups present in the supernatant solution of the bacteria that participated Reducing AgNO3 and converting it into silver nanoparticles and preventing the oxidation process of these particles, in addition to their encapsulating and stabilizing action, which contributed to the stability of the particles in the long term [38].

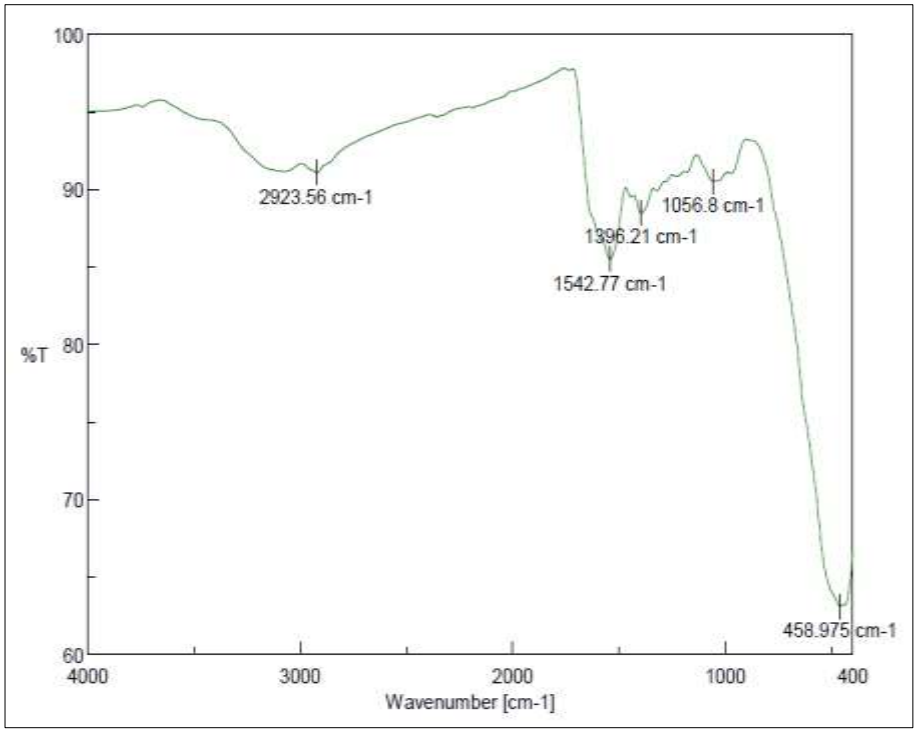

Fig 7: FTIR of silver nanoparticles formed by *B. subtilis* supernatant. The spectrum of FTIR identified the unique peaks at 2923.56 cm^{-1}, 1542.77 cm^{-1}, 1396.21 cm^{-1}, and 1056.8 $cm.^{-1}$

Examination using SEM and TEM

The results of the examination using SEM showed that the silver nanoparticles had multiple shapes, with the spherical shape predominant, and the diameters of the particles ranged from 37.38 to 14.66 nm with an average of 26.31 nm. The TEM result also showed that the spherical shape was dominant among the shapes, with sizes (42.72-13.77 nm) and a rate of 25.29 nm, as shown in Figure (8). The results were consistent with many studies using theupernatant solution of bacteria to create silver nanoparticles [39].

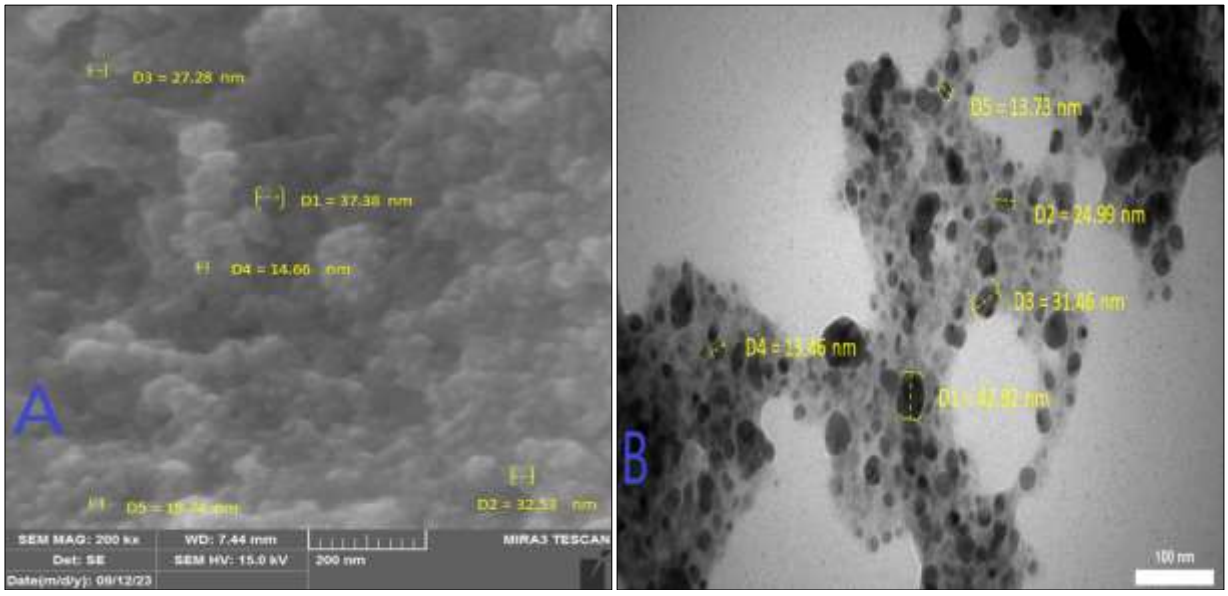

Fig 8: The results of the examination using SEM showed that the silver nanoparticles had multiple shapes, with the spherical shape predominant, and the diameters of the particles ranged from 37.38 to 14.66 nm with an average of 26.31 nm. The TEM result also showed that the spherical shape was dominant among the shapes, with sizes (42.72-13.77 nm) and a rate of 25.29 nm, The results were consistent with many studies using the floating solution of bacteria to create silver nanoparticles

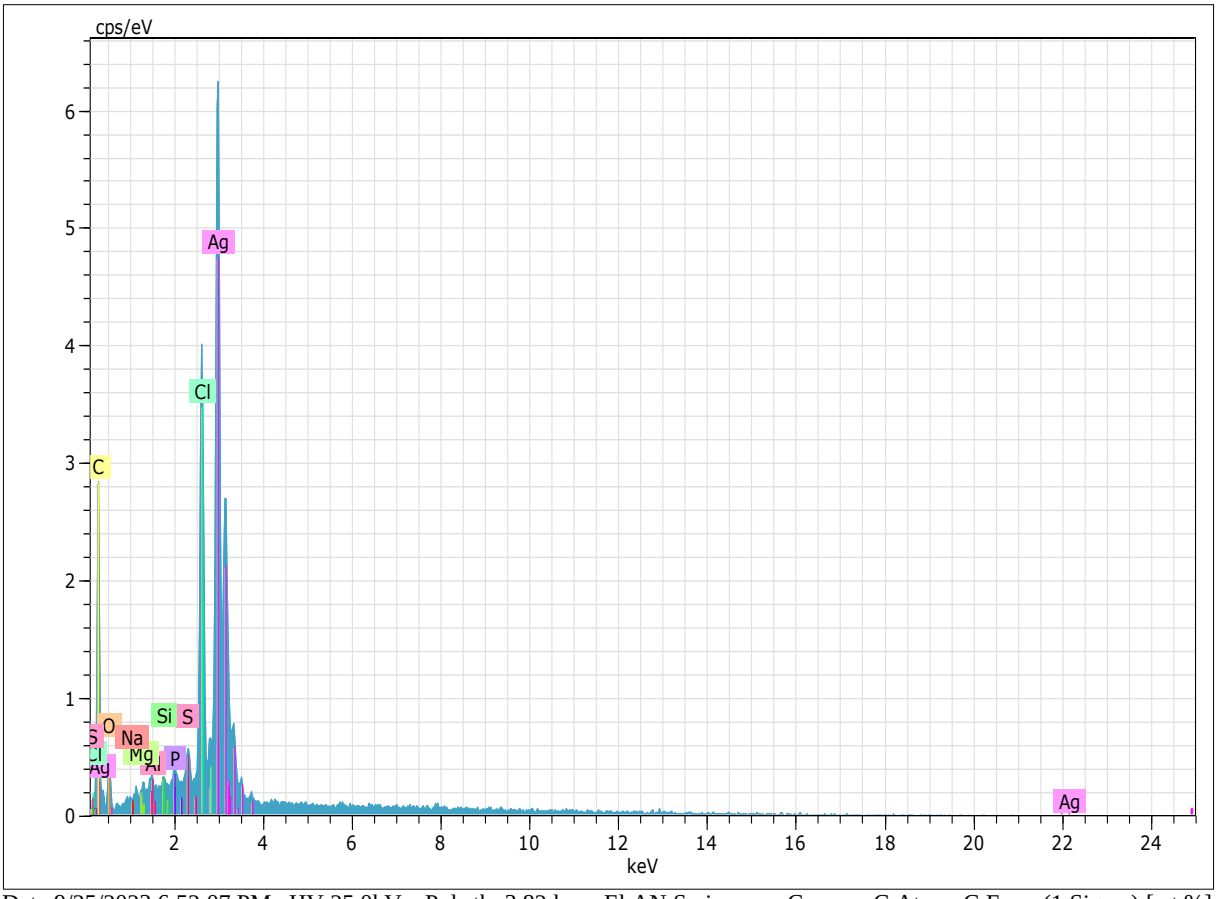

Date:9/25/2023 6:52:07 PM HV:25.0kV Puls th.:3.82 kcps El AN Series unn. C norm. C Atom. C Error (1 Sigma) [wt.%] [wt.%] [at.%] [wt.%]
Ag 47 L-series 45.48 40.74 8.40 1.51
C 6 K-series 12.24 9.84 70.07 7.44
O 8 K-series 11.11 9.95 13.83 3.12
Cl 17 K-series 9.44 8.45 5.30 0.38
S 16 K-series 0.99 0.89 0.62 0.08
P 15 K-series 0.63 0.56 0.41 0.07
Al 13 K-series 0.60 0.54 0.45 0.08
Mg 12 K-series 0.43 0.39 0.36 0.08
Na 11 K-series 0.43 0.38 0.37 0.09
Si 14 K-series 0.28 0.25 0.20 0.05
Total: 81.62 71.00 100.00

Fig 9: The EDX spectrum recorded from a film after the formation of silver nanoparticles. Different X-ray emission peaks are labeled

Energy Dispersive X-ray Spectroscopy (EDX)

The result of the EDX examination showed that the silver nanoparticles were created by the supernatant solution of *B. subtilis* bacteria. The examination result showed that the powder of the silver nanoparticles contained the element silver at a percentage of 45.48 out of a total of 81.62, in addition to the elements C and O, where the percentage of each of them reached 12.24 and 11.11, respectively. Respectively, the reason for the presence of O and C is due to the exposure of silver nanoparticle powder to atmospheric conditions in the laboratory. As for the rest of the elements, the reason for the presence of some of them may be due to the nature of biosynthesis, as the supernatant solution of the bacteria originally contains these elements, in addition to the presence of some elements in the water that was used to wash the extract of silver nanoparticles after extracting them from the reaction mixture, as shown in Figure 9 [40].

X-ray diffraction (XRD)

Silver nanoparticles by *B. subtilis* prepared by were examined using an XRD device within an angular range of (2) (80-10) to detect the crystalline and structural properties of nanomaterials, the results showed that silver nanoparticles have X-ray diffraction represented by peaks (111), (200), (202), and (311) at angles (38.20176°), (46.6°), (65.2°), and (77.47°) Respectively, when compared with the JCPDS card 00-00-40783, the results show that the silver nanoparticles have a face-centered cubic shape, as in Figure 10 [41].

Antimicrobial activity of AgNPs

The results of the current study showed that biosynthetic silver nanoparticles have an effective effect on the growth of pathogenic bacteria, as AgNPs gave varying diameters of inhibition when using different concentrations. They gave the largest diameter of inhibition on *P. aeruginosa* bacteria, as the diameter of inhibition reached 21 mm at 100% concentration. The smallest diameter of inhibition was for *E. coli* bacteria, reaching 12 mm at a concentration of 25%. The results showed that silver nanoparticles in their different concentrations have the ability to inhibit the growth of pathogenic bacteria in different proportions, as shown in

Table 4 and. Image 7 The results of the table showed that inhibition of bacterial growth occurred clearly at high concentrations, and the results showed that there were differences between the diameters of inhibition between the bacterial isolates, which is due to the difference in the composition of the bacterial wall, cell physiology in general, and genetic makeup, in addition to the enzymes that play an important role. In cellular metabolism Table 4 Figure 11 [42].

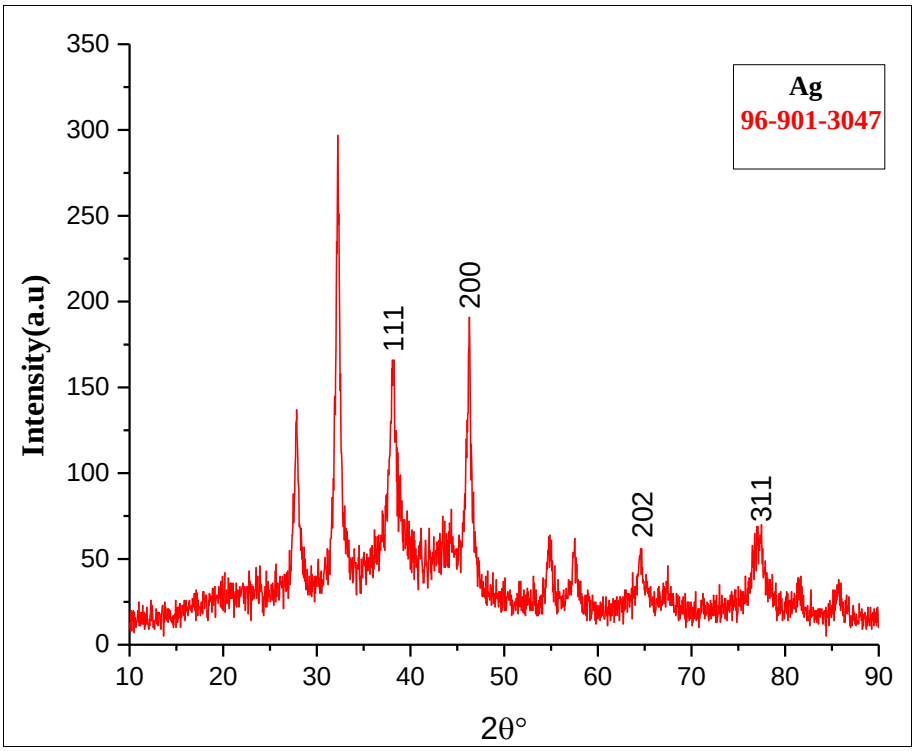

Fig 10: XRD of silver nanoparticles formed by *Bacillus subtilis* supernatant. The XRD patterns at 2 θ values 38.2°-46.6°-65.2°- 77.47° indicated the reflections of metallic silver

Table 4: Inhibition Zone (mm) on Pathogenic Bacteria

Inhibition zone (mm) on Pathogenic Bacteria				Pathogenic bacteria
Concentration 100 µg \ ml	**Concentration 75 µg \ ml**	**Concentration 50 µg \ ml**	**Concentration 25 µg \ ml**	
21 mm	19.5 mm	15.5 mm	14.5 mm	*P. aeruginosa*
14.5 mm	14 mm	12.75 mm	12 mm	*E. coli*
17 mm	15.5 mm	14.5 mm	13.25 mm	*K. pneumonia*
16 mm	15 mm	15 mm	14 mm	*S. aureus*

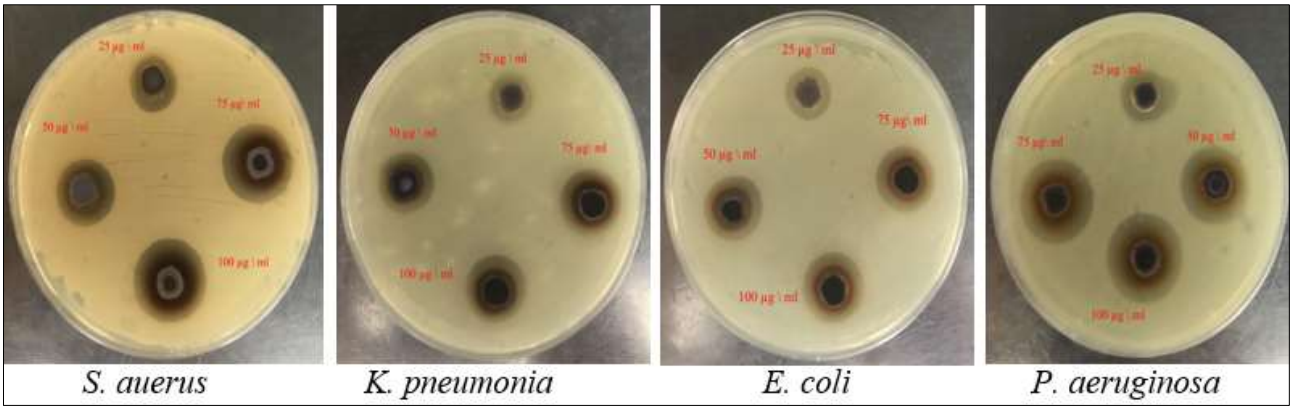

Fig 11: Effect of AgNPs on pathogenic bacteria A- *P. aeruginosa*; B-E. - *E. coli* C- *K. pneumonia* D- *S. aureus* with concentrations (25-50 - 75-100 µg/mL)

Minimum inhibitory concentration (MIC): The MIC results for *P. aeruginosa E. coli* K. pneumonia bacteria showed that it was 25 µg\ml while it was 50 µg\ml for *S. aureus* bacteria, as in the Figure (12) [43].

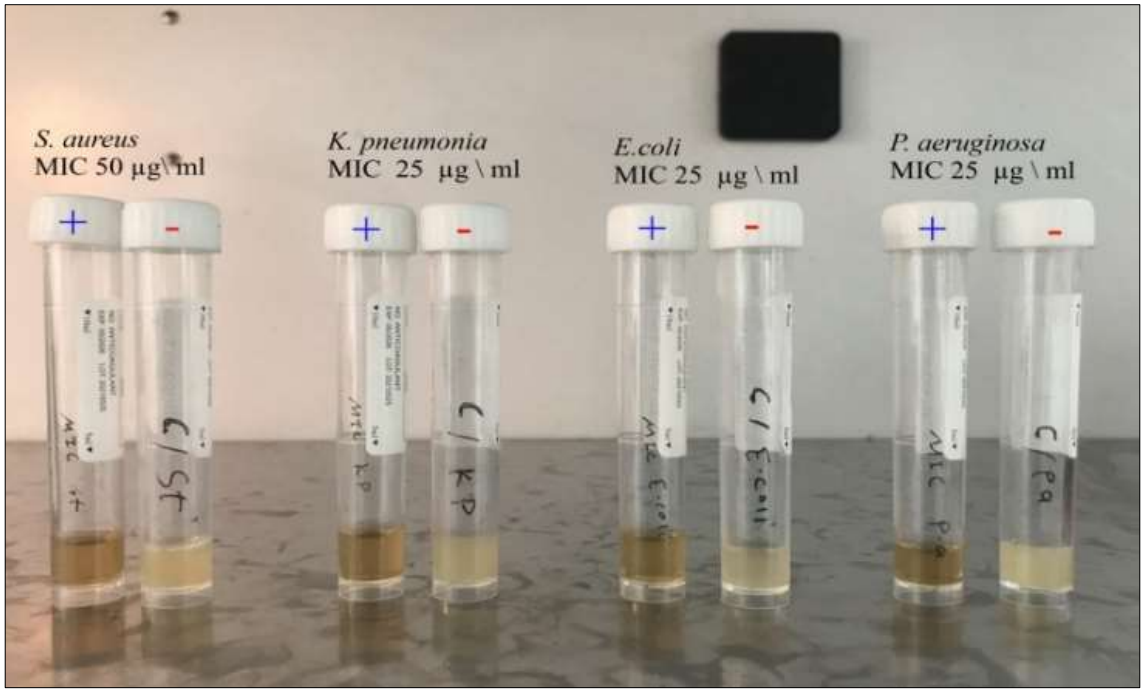

Fig 12: The minimum inhibitory concentration (MIC)

Inhibition of catalase

The results of the examination showed that silver nanoparticles with varying concentrations, as shown in Table 4, had the ability to inhibit the production of the catalase enzyme in pathogenic bacteria, which is one of the virulence factors in bacteria, as the bacteria use it as one of the virulence factors, as this enzyme works to decompose hydrogen peroxide into oxygen and water. This enzyme plays an important role in protecting cells from oxidative stress resulting from the formation of reactive oxygen species (ROS), as the catalase enzyme works to overcome oxidative stress and silver nanoparticles work, due to their small size and positive charge, to penetrate bacterial cells and interfere with biological molecules, thus leading to a reduction and absence of catalase production Figure 13 and Table 5 [44].

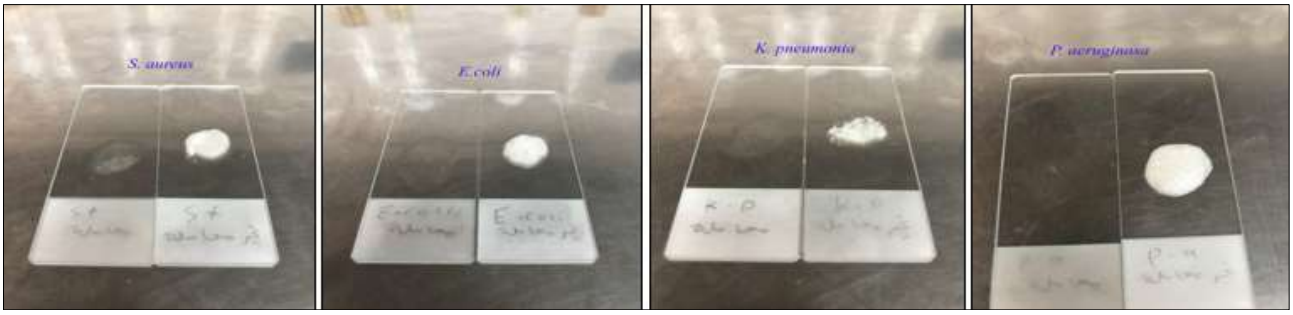

Fig 13: Inhibition catalase

Table 5: Concentrations of AgNPs on pathogenic bacteria inhibition catalase

Inhibition concentration catalase	Isolate
50 µg\ ml	*P. aeruginosa*
25 µg \ ml	*E. coli*
25 µg \ ml	*K. pneumonia*
50 µg \ ml	*S. aureus*

Biofilm formation by pathogenic bacteria in a microliter plate: The intensity of biofilm formation in pathogenic bacteria was calculated by comparing the absorbance result of the negative control hole (control -) AC, which contains the culture medium only, with the absorbance result of the positive control hole (control +) A, which contains the culture medium with the bacterial suspension of the biofilm-forming bacteria. The results showed that all bacterial isolates isolated from disease cases formed a biofilm to a high degree, and Table 6 and Figure 14 show the intensity of biofilm formation [45].

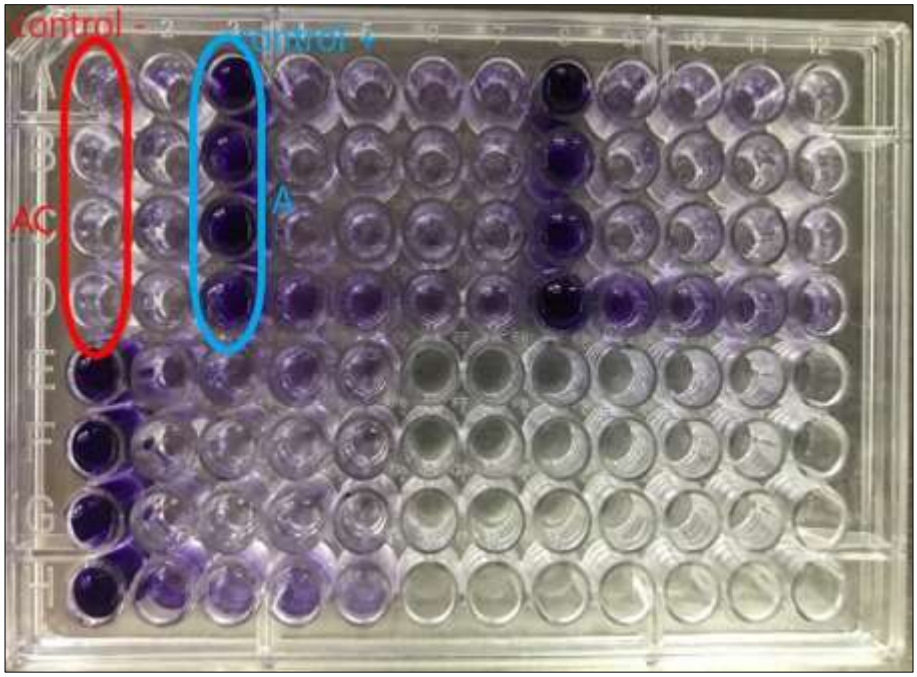

Fig 14: Shows the intensity of biofilm formation on the microtiter plate

Table 6: Calculating the intensity of biofilm formation in pathogenic bacteria

Biofilm response	Biofilm Formation		Isolates
strongly biofilm	2 * 0.071 ≤ 1.135	2 * AC ≤ A	*P. aeruginosa*
strongly biofilm	2 * 0.070 ≤ 0.881	2 * AC ≤ A	*E. coli*
strongly biofilm	2 * 0.068 ≤ 1.484	2 * AC ≤ A	*K. pneumonia*
strongly biofilm	2 * 0.066 ≤ 0.962	2 * AC ≤ A	*S. aureus*

Effect of silver nanoparticles on biofilm formation in a microtiter plate

The inhibition force of AgNPs on the biofilm was calculated by applying the equation for calculating the inhibition force. The pits forming the biofilm were considered negative control pits, and the rest of the pits containing AgNP concentrations were considered positive control pits. When the equation was applied, it was shown that the highest percentage of inhibition found on *S. aureus* was 93.40% at a concentration of 100 µg/ml, and the lowest percentage of inhibition found on *S. aureus* was 83.47% at a concentration of 25 µg/ml with a probability level of 0.05, as shown in Table 7 and the. Figure (15) The results were consistent with [46].

Table 7: Inhibition rates of silver nanoparticles and significant differences between the concentrations used to inhibit biofilm

Average effect of silver nanoparticles	Average type of bacteria	Concentrations of silver nanoparticles				Types of bacteria
		100 µg \ ml	75 µg \ ml	50 µg \ ml	25 µg \ ml	
88.05	87.80	88.53%	88.10%	87.77%	86.80%	*P. aeruginosa*
89.79	90.38	91.00%	90.03%	89.40%	91.07%	*E. coli*
90.49	91.63	92.57%	91.80%	91.30%	90.87%	*K. pneumonia*
91.37	89.90	93.40%	92.03%	90.70%	83.47%	*S. aureus*
4.506 Bilateral interference		LSD 2.253 silver nanoparticles			LSD 2.253 bacteria	

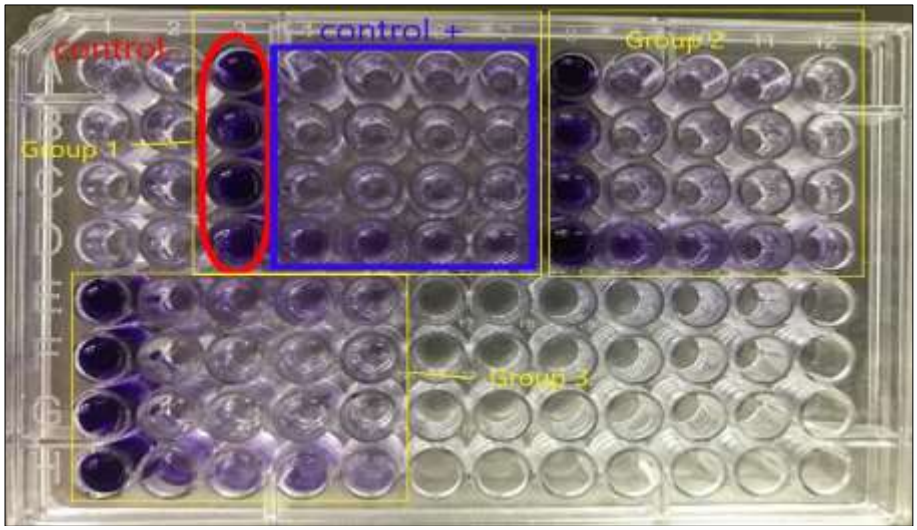

Fig 15: Groups (1, 2, - 3) containing negative and positive control factors

Conclusion

The results of the current study demonstrated the high ability of *Bacillus subtilis* bacteria to synthesize silver nanoparticles by using the supernatant solution of the bacteria. The tests used to characterize the silver nanoparticles showed that they were of multiple shapes, with a predominant spherical shape, and the sizes of the silver nanoparticles ranged from 14 to 42 nm at a rate of 25 nm. The results of its use against pathogenic bacteria showed that it has a very high ability to inhibit the growth of pathogenic bacterial isolates the results of using silver nanoparticles against biofilm formation and catalase production in bacterial isolates showed that they have a high level of ability to inhibit catalase production and biofilm formation. Therefore, silver nanoparticles can be used in the future to develop drugs against multi-resistant bacterial infections.

References

1. Mulani MS, Kamble EE, Kumkar SN, Tawre MS, Pardesi KR. Emerging strategies to combat ESKAPE pathogens in the era of antimicrobial resistance: A review. Frontiers in Microbiology. 2019;10:539.
2. Bedlovicová Z, Salayová A. Green-synthesized silver nanoparticles and their potential for antibacterial applications. Bacterial Pathogenesis and Antibacterial Control; c2017.
3. Hemlata, Meena PR, Singh AP, Tejavath KK. Biosynthesis of silver nanoparticles using *Cucumis prophetarum* aqueous leaf extract and their antibacterial and antiproliferative activity against cancer cell lines. ACS Omega. 2020;5(10):5520-5528.
4. Jagielski T, Bakuła Z, Pleń M, Kamiński M, Nowakowska J, Bielecki J, *et al*. The activity of silver nanoparticles against microalgae of the *Prototheca* genus. Nanomedicine. 2018;13(9):1025-1036.
5. Qais FA, Shafiq A, Ahmad I, Husain FM, Khan RA, Hassan I, *et al*. Green synthesis of silver nanoparticles using *Carum copticum*: Assessment of its quorum sensing and biofilm inhibitory potential against gram-negative bacterial pathogens. Microbial Pathogenesis. 2020;144:104172.
6. Soleimani M, Habibi-Pirkoohi M. Biosynthesis of silver nanoparticles using *Chlorella vulgaris* and evaluation of the antibacterial efficacy against *Staphylococcus aureus*. Avicenna Journal of Medical Biotechnology. 2017;9(3):120.
7. Khateef R, Khadri H, Almatroudi A, Alsuhaibani SA, Mobeen SA, Khan RA, *et al*. Potential in-vitro anti-breast cancer activity of green-synthesized silver nanoparticles preparation against human MCF-7 cell-lines. Advances in Natural Sciences: Nanoscience and Nanotechnology. 2019;10(4):045012.
8. Ahmed T, Shahid M, Noman M, Niazi MBK, Mahmood F, Manzoor I, *et al*. Silver nanoparticles synthesized by using *Bacillus cereus* SZT1 ameliorated the damage of bacterial leaf blight pathogen in rice. Pathogens. 2020;9(3):160.
9. Almalki MA, Khalifa AY. Silver nanoparticles synthesis from *Bacillus* sp. KFU36 and its anticancer effect in breast cancer MCF-7 cells via induction of apoptotic mechanism. Journal of Photochemistry and Photobiology B: Biology. 2020;204:111786.
10. Roy A, Bulut O, Some S, Mandal AK, Yilmaz MD. Green synthesis of silver nanoparticles: Biomolecule-nanoparticle organizations targeting antimicrobial activity. RSC Advances. 2019;9(5):2673-2702.
11. Ovais M, Khalil AT, Ayaz M, Ahmad I, Nethi SK, Mukherjee S, *et al*. Biosynthesis of metal nanoparticles via microbial enzymes: A mechanistic approach. International Journal of Molecular Sciences. 2018;19(12):4100.
12. Saravanan M, Barik SK, MubarakAli D, Prakash P, Pugazhendhi A. Synthesis of silver nanoparticles from *Bacillus brevis* (NCIM 2533) and their antibacterial activity against pathogenic bacteria. Microbial Pathogenesis. 2018;116:221-226.
13. Alshami HGA, AL-Tamimi WH, Hateet RR. Screening for extracellular synthesis of silver nanoparticles by bacteria isolated from Al-Halfaya oil field reservoirs in Missan province, Iraq. Biodiversitas Journal of Biological Diversity, 2022, 23(7).
14. Al-Dahmoshi HOM. Genotypic and phenotypic investigation of alginate biofilm formation among *Pseudomonas aeruginosa* isolated from burn victims in Babylon, Iraq. Science Journal of Microbiology; c2013.
15. Varela-Rodríguez EN, Arvizu-Gómez JL, Martínez-Rizo AB, González-Reyes C. Molecular identification of *Pseudomonas aeruginosa* and antibiotic resistance testing. GSC Biological and Pharmaceutical Sciences. 2023;24(2):308-316.
16. Obaid HM. In Vitro assessment of biosynthesized silver nanoparticles effect on some intestinal protozoan cystic stages. International Journal of Biology Research. 2022;7(3):22-27.
17. Medda S, Hajra A, Dey U, Bose P, Mondal NK. Biosynthesis of silver nanoparticles from *Aloe vera* leaf extract and antifungal activity against *Rhizopus* sp. and *Aspergillus* sp. Applied Nanoscience. 2015;5:875-880.
18. Bachii SA, Abd-Al Sahib WH. Preparation and characterization of silver nanoparticles biosynthesis by *Pseudomonas stutzeri* environmental bacteria isolated from oil fields and their antimicrobial activity.
19. Almatroudi A. Silver nanoparticles: Synthesis, characterisation and biomedical applications. Open Life Sciences. 2020;15(1):819-839.
20. Shareef AA, Alriyahee FAA, Hasan ZA, Kadhim MA, Al-Mussawi AA. Biogenic synthesis of silver nanoparticles by *Sedilitizia rosmarinus boiss* shoot extract and its antibacterial activity against MDR bacteria. Turkish Journal of Physiotherapy and Rehabilitation, 2023, 32(3).
21. Ghiuță I, Cristea D, Croitoru C, Kost J, Wenkert R, Vyrides I, *et al*. Characterization and antimicrobial activity of silver nanoparticles, biosynthesized using *Bacillus* species. Applied Surface Science. 2018;438:66-73.
22. Almatroudi A. Silver nanoparticles: Synthesis, characterisation and biomedical applications. Open Life Sciences. 2020;15(1):819-839.
23. Neethu S, Midhun SJ, Sunil MA, Soumya S, Radhakrishnan EK, Jyothis M, *et al*. Efficient visible light induced synthesis of silver nanoparticles by *Penicillium polonicum* ARA 10 isolated from *Chaetomorpha antennina* and its antibacterial efficacy against *Salmonella enterica* serovar Typhimurium.

Journal of Photochemistry and Photobiology B: Biology. 2018;180:175-185.
24. Bakht Dalir SJ, Djahaniani H, Nabati F, Hekmati M. Characterization and the evaluation of antimicrobial activities of silver nanoparticles biosynthesized from *Carya illinoinensis* leaf extract. Heliyon, 2020, 6(3).
25. Devi JS, Bhimba BV, Ratnam K. In vitro anticancer activity of silver nanoparticles synthesized using the extract of *Gelidiella* sp. International Journal of Pharmaceutical Sciences and Research. 2012;4(4):710-715.
26. Ahmad A, Wei Y, Syed F, Tahir K, Rehman AU, Khan A, *et al*. The effects of bacteria-nanoparticles interface on the antibacterial activity of green synthesized silver nanoparticles. Microbial Pathogenesis. 2017;102:133-142.
27. Patil SV, Borase HP, Patil CD, Salunke BK. Biosynthesis of silver nanoparticles using latex from few euphorbian plants and their antimicrobial potential. Applied Biochemistry and Biotechnology. 2012;167:776-790.
28. Ali OAU. Prevention of *Proteus mirabilis* biofilm by surfactant solution. Egyptian Academic Journal of Biological Sciences, G. Microbiology. 2012;4(1):1-8.
29. MacFaddin JF. *B*iochemical Tests for Identification of Medical Bacteria. Williams and Wilkins; Philadelphia, PA; c2000.
30. Colle J, Fraser A, Marmion P, Simmans A. Mackia Macartnre Practical Medical Microbiology 14th Ed. Churchill Livingstone. New York; c1996.
31. Murray RG, Holt JG. The history of Bergey's Manual. In: Bergey's Manual® of Systematic Bacteriology. Springer; c2005. p. 1-14.
32. Holt JG, Krieg NR, Sneath PH, Staley JT, Williams ST. Bergey's Manual of Determinative Bacteriology. Lippincott Williams & Wilkins; c1994.
33. González MJ, Gorgoroso F, Reginensi SM, Olivera JA, Bermúdez J. Polyphasic identification of closely related *Bacillus subtilis* and *Bacillus amyloliquefaciens* isolated from dairy farms and milk powder. Journal of Microbiology, Biotechnology and Food Sciences. 2013;2(5):2326-2331.
34. Al-Dhabaan FA. Morphological, biochemical and molecular identification of petroleum hydrocarbons biodegradation bacteria isolated from oil polluted soil in Dhahran, Saudi Arabia. Saudi Journal of Biological Sciences. 2019;26(6):1247-1252.
35. Ranganath E, Rathod V, Banu A. Screening of *Lacto Bacillus* spp. for mediating the biosynthesis of silver nanoparticles from silver nitrate. IOSR Journal of Pharmacy. 2012;2(2):237-241.
36. Ahmed T, Shahid M, Noman M, Niazi MBK, Mahmood F, Manzoor I, *et al*. Silver nanoparticles synthesized by using *Bacillus cereus* SZT1 ameliorated the damage of bacterial leaf blight pathogen in rice. Pathogens. 2020;9(3):160.
37. Shankar SS, Ahmad A, Sastry M. Geranium leaf assisted biosynthesis of silver nanoparticles. Biotechnology Progress. 2003;19(6):1627-1631.
38. Kumar D, Kumar G, Agrawal V. Green synthesis of silver nanoparticles using *Holarrhena antidysenterica* (L.) Wall. bark extract and their larvicidal activity against dengue and filariasis vectors. Parasitology Research. 2018;117:377-389.
39. Deljou A, Goudarzi S. Green extracellular synthesis of the silver nanoparticles using thermophilic *Bacillus* sp. AZ1 and its antimicrobial activity against several human pathogenetic bacteria. Iranian Journal of Biotechnology. 2016;14(2):25.
40. Kumar CG, Mamidyala SK. Extracellular synthesis of silver nanoparticles using culture supernatant of *Pseudomonas aeruginosa*. Colloids and Surfaces B: Biointerfaces. 2011;84(2):462-466.
41. Selvaraj V, Sagadevan S, Muthukrishnan L, Johan MR, Podder J. Eco-friendly approach in synthesis of silver nanoparticles and evaluation of optical, surface morphological and antimicrobial properties. Journal of Nanostructure in Chemistry. 2019;9:153-162.
42. Shareef HA, Jafar NB, Abdulrahman RB. The Biosynthesis of Silver Nanoparticles by *Moringa Oleifera* and its Antibacterial Activity. Indian Journal of Public Health Research & Development, 2019, 10(8).
43. Hamida RS, Ali MA, Goda DA, Khalil MI, Al-Zaban MI. Novel biogenic silver nanoparticle-induced reactive oxygen species inhibit the biofilm formation and virulence activities of methicillin-resistant *Staphylococcus aureus* (MRSA) strain. Frontiers in Bioengineering and Biotechnology. 2020;8:433.
44. Roy S, Das TK. Effect of biosynthesized silver nanoparticles on the growth and some biochemical parameters of *Aspergillus foetidus*. Journal of Environmental Chemical Engineering. 2016;4(2):1574-1583.
45. Liew SM, Rajasekaram G, Puthucheary SA, Chua KH. Antimicrobial susceptibility and virulence genes of clinical and environmental isolates of *Pseudomonas aeruginosa*. Peer J; c2019. p. 7.
46. Salomoni R, Léo P, Montemor AF, Rinaldi BG, Rodrigues MFA. Antibacterial effect of silver nanoparticles in *Pseudomonas aeruginosa*. Nanotechnology, Science and Applications; c2017. p. 115-121.